Endogenous Sheet-Averaged Tension Within a Large Epithelial Cell Colony

Sandeep P. Dumbali
Mechanical and Aerospace Engineering,
Old Dominion University,
Norfolk, VA 23529

Lanju Mei
Mechanical and Aerospace Engineering,
Old Dominion University,
Norfolk, VA 23529

Shizhi Qian
Mechanical and Aerospace Engineering,
Old Dominion University,
Norfolk, VA 23529

Venkat Maruthamuthu[1]
Mechanical and Aerospace Engineering,
Old Dominion University,
4635 Hampton Boulevard,
238e Kaufman,
Norfolk, VA 23529
e-mail: vmarutha@odu.edu

Epithelial cells form quasi-two-dimensional sheets that function as contractile media to effect tissue shape changes during development and homeostasis. Endogenously generated intrasheet tension is a driver of such changes, but has predominantly been measured in the presence of directional migration. The nature of epithelial cell-generated forces transmitted over supracellular distances, in the absence of directional migration, is thus largely unclear. In this report, we consider large epithelial cell colonies which are archetypical multicell collectives with extensive cell–cell contacts but with a symmetric (circular) boundary. Using the traction force imbalance method (TFIM) (traction force microscopy combined with physical force balance), we first show that one can determine the colony-level endogenous sheet forces exerted at the midline by one half of the colony on the other half with no prior assumptions on the uniformity of the mechanical properties of the cell sheet. Importantly, we find that this colony-level sheet force exhibits large variations with orientation—the difference between the maximum and minimum sheet force is comparable to the average sheet force itself. Furthermore, the sheet force at the colony midline is largely tensile but the shear component exhibits significantly more variation with orientation. We thus show that even an unperturbed epithelial colony with a symmetric boundary shows significant directional variation in the endogenous sheet tension and shear forces that subsist at the colony level. [DOI: 10.1115/1.4037404]

Keywords: epithelial colony, traction force, endogenous sheet tension, cell–cell contact

1 Introduction

The contractility of epithelial cells and the transmission of endogenous cell-generated forces over supracellular distances are important drivers of morphological changes at the tissue-level and beyond [1,2]. In fact, epithelial sheets can use biochemical cues to break in-plane symmetry and generate anisotropic endogenous tension [3]. However, the nature of supracellular force transmission in epithelial sheets, even in the absence of developmental cues, is largely unclear. In this regard, in vitro cell collectives such as cell colonies, in spite of their limited size and presence of free boundary, are an accessible model system to understand the fundamental nature of endogenous forces and how they are transmitted in a multicellular context.

Cell-generated forces are transmitted through multicellular epithelial sheets via cell–cell contacts bound by cell–cell adhesion structures, such as adherens junctions [4]. Forces transmitted through epithelial cell–cell contacts have been measured using multiple techniques local to the cell–cell contact [5–7] by using molecular tension sensors, oil droplets, and laser ablation. On the other hand, traction force microscopy-based methods [8–13] have provided a complementary picture with quantitative measures of cellular force generation and transmission in single cells, small islands, and expanding monolayers. However, our knowledge of force transmission in quiescent, large epithelial cell colonies is limited.

While multiple studies have reported on forces transmitted in small islands of two or more cells [8,9,14,15], studies on monolayers [12] have provided information on local forces, but with assumptions such as homogeneous cell mechanical properties across the monolayer. However, the dependence of cell stiffness on cell prestress suggests that cell mechanical properties may not be homogeneous across cell sheets [16]. Here, we consider a large epithelial cell colony (large in the sense that the extent of cell–cell contacts is much larger than the free cell colony boundary) that is also circular in shape. While the effect of the free boundary is itself not eliminated, the circular shape does eliminate directional cues due to asymmetric free boundaries. Without assuming uniform cell mechanical properties, while we cannot obtain local forces, we demonstrate that the endogenous forces within the cell sheet can be determined at the whole epithelial colony level. We also uncover significant variation of this large tensile force with orientation.

2 Methods

2.1 Cell Culture. Dulbecco's modified Eagle's medium (Corning Inc., Corning, NY) supplemented with L-glutamine, sodium pyruvate, 1% Penicillin/streptomycin, and 10% fetal bovine serum (Corning Inc., Corning, NY) was used to grow Madin Darby canine kidney (MDCK) cells under 5% CO_2. For plating micropatterned polyacrylamide (PAA) hydrogels, about 10^5 cells were plated on 35-mm culture dishes with hydrogels and the medium was replaced within 0.5 h after plating.

2.2 Preparation and Micropatterning of Polyacrylamide Hydrogel Substrates. Polyacrylamide gels were made with an acrylamide to bisacrylamide ratio of 7.5%:0.1%. Red fluorescent beads of diameter 0.44 μm (Spherotech Inc., Lake Forest, IL) were included as fiducial markers. For micropatterning the PAA gels [17], a 22 mm × 22 mm glass coverslip (no. 1.5) was first treated with deep UV light to render it hydrophilic. The coverslip was then incubated with a solution of 0.1 mg/ml poly(L-lysine)-poly(ethylene glycol) at *p*H 7.4 for 30 min. Then, it was exposed to deep UV light with a quartz chrome photomask (Toppan, Round Rock, TX) (with the 500 μm clear circle in the light path) for 5 min. The coverslip was then incubated with 0.02 mg/ml collagen 1 protein (at *p*H 8.5) for 30 min. The PAA gel was then polymerized sandwiched between the collagen-coated coverslip

[1]Corresponding author.

Manuscript received March 16, 2017; final manuscript received July 21, 2017; published online August 18, 2017. Assoc. Editor: Jeffrey Ruberti.

and an activated coverslip (activated by treating successively with 2% 3-aminopropyltrimethyoxysilane in isopropanol and 1% glutaraldehyde in distilled water). The resultant PAA gel had a thickness of ~150 μm as determined from z-stacks of images of fluorescent beads within the gel.

2.3 Traction Force Measurements. An imaging system consisting of a Leica DMi8 epifluorescence microscope (Leica Microsystems, Buffalo Grove, IL) with a 10×0.3 NA objective, HQ2-cooled CCD camera (Photometrics, Tucson, AZ) and an airstream incubator (Nevtek, Williamsville, VA) was used to obtain phase images of MDCK cell colonies and red bead images (from the top surface of the gel) beneath them. Bead images were also obtained after the colonies were removed using 10% sodium dodecyl sulfate. After image alignment using Image J [18], the displacement of the beads was calculated using MATLAB (MathWorks, Natick, MA) with code available at the website.[2] Traction forces were then reconstructed from the displacements of the gel surface using regularized Fourier transform traction cytometry which employs the Boussinesq solution [19–22].

2.4 Sheet Force Calculations. The epithelial sheet force at the colony midline was calculated similar to what was implemented for TFIM of cell pairs previously [9], except that the colony midline demarcated the two parts of the colony here. A binary mask (dilated by 10%) based on the micropattern diameter (0.5 mm) was used to select all the traction forces exerted by the colony (to calculate the scalar sum $\Sigma(\text{colony})|\mathbf{T_i}|$ or vector sum $\Sigma(\text{colony})\mathbf{T_i}$) so that noise contributions from regions away from the colony and that due to the frame boundary are avoided. Two half masks on either side of the colony midline (which in turn was constructed at an angle θ with respect to the horizontal) were used to select traction forces exerted by the two halves of the colony. The sheet force exerted on half 1 (by the other half, half 2) is $\mathbf{F_{12}} = \Sigma(\text{half1})\mathbf{T_i}$ and the sheet force exerted on half 2 (by the other half, half 1) is $\mathbf{F_{21}} = \Sigma(\text{half2})\mathbf{T_i}$. The sheet force $\mathbf{F}_{\text{sheet}}$ is thus the average $(\mathbf{F_{12}} - \mathbf{F_{21}})/2$ (the difference is used as $\mathbf{F_{12}}$ is directed roughly opposite to $\mathbf{F_{21}}$), with an associated error of $(\mathbf{F_{12}} + \mathbf{F_{21}})/2$ (as explained in Ref. [9]). If the angle made by the sheet force to the colony midline is α, the sheet tension at the midline is $\mathbf{F}_{\text{sheet}} \sin\alpha$ and the sheet shear is $\mathbf{F}_{\text{sheet}} \cos\alpha$. All the binary masks were created using ImageJ and all the force calculations mentioned earlier were using custom-written scripts in MATLAB (MathWorks, Natick, MA).

2.5 Finite Thickness Traction Computation. The traction force under the epithelial cell colony was also computed (from the experimentally measured displacement field) taking into account the finite thickness of the substrate using a commercial finite element package, COMSOL. For this, substrate of dimensions width 3 mm, length 3 mm, and height 150 μm was assumed, with the experimentally measured displacement field applied on the top surface and the bottom surface fixed (zero displacement). We assumed hydrogel properties of Young's modulus 13.5 kPa and Poisson's ratio 0.49. Tetrahedral mesh was employed with denser mesh on the top surface where the displacement field is imposed, with a total of 38,423 units in the mesh. The system was numerically solved using the Solid Mechanics module in COMSOL MULTIPHYSICS (COMSOL Inc., Burlington, MA) and the computation was carried out on a high performance computing cluster at ODU, Norfolk, VA.

3 Results

We micropatterned collagen I as a half millimeter-wide filled circle on PAA gel and then plated MDCK cells on them resulting in a cohesive circular epithelial cell colony (Figs. 1(*a*) and 1(*b*)).

[2] http://www.oceanwave.jp/softwares/mpiv/

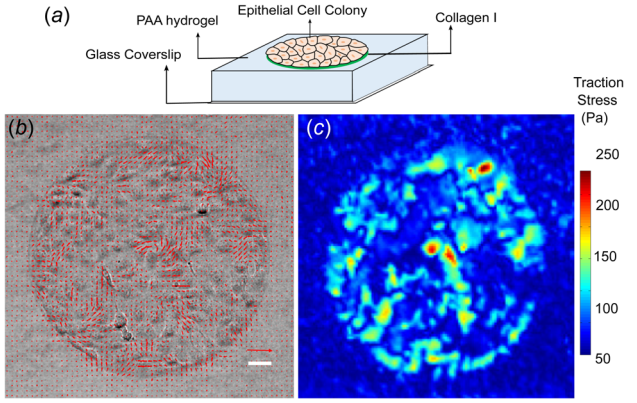

Fig. 1 (*a*) Schematic depiction of the epithelial cell colony on the PAA hydrogel. (*b*) Phase image of the circular MDCK cell colony with the traction stress vectors overlaid. Scale bar for distance is 50 μm and for traction vector is 1000 Pa. (*c*) Heat map representation of the traction stress under the colony.

Using TFIM, which has previously been used to determine the endogenous force exerted at a single cell–cell contact, we sought to determine the endogenous sheet force exerted within a large epithelial cell colony. Here, based on the position of submicron fluorescent beads in the PAA gel with and without the colony on it, we first determined the displacement field of the gel under the cell colony using particle image velocimetry and then computed the traction force field using regularized Fourier transform traction cytometry [9,21,22]. The traction stress field is depicted superimposed on the phase image of the epithelial cell colony in Fig. 1(*b*), with the corresponding traction stress heat map in Fig. 1(*c*).

The epithelial cell colony we consider exerts traction forces in a manner qualitatively different from small cell islands considered in many previous studies. While small cell islands (wherein the extent of free edge boundaries are comparable to that of cell–cell contacts) have been previously shown to predominantly exert large traction stresses only near the islands edges [9,11,14,15], the larger colony considered here (wherein the contour length of free edge boundary is much less than the contours of all the cell–cell contacts within the colony) exerts large traction stresses at the edges as well as in the interior regions of the colony (Fig. 1(*c*)). In fact, when we considered above average traction stresses as a proxy for large traction stresses, we found that their frequency distribution (Fig. 2(*a*)) was similar in the central, medial, and distal

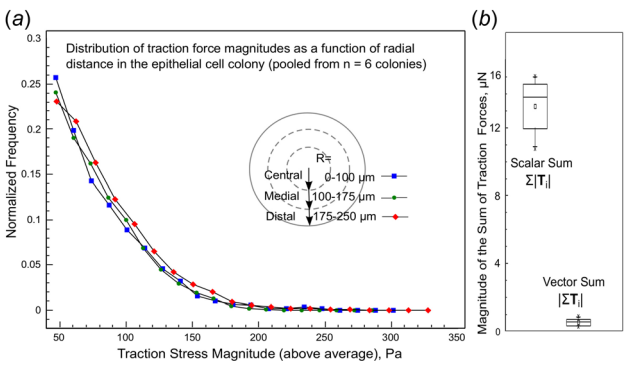

Fig. 2 (*a*) Distribution of the magnitudes of traction stresses exerted under the central, medial, and distal regions within the colonies. Only above average traction stresses (used as a proxy for significant/large traction stresses) are considered in this plot. Data are pooled from $n = 6$ colonies. (*b*) Traction forces under each epithelial cell colony are balanced. The vector sum for each of the colonies is close to zero relative to the scalar sum of the traction forces that are shown for comparison. $n = 6$ colonies.

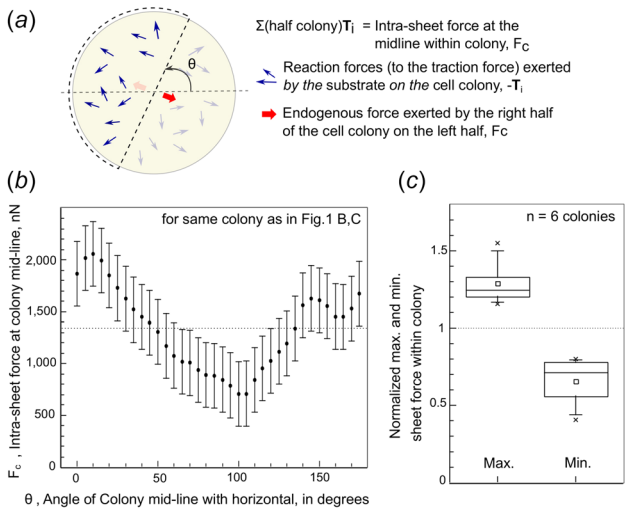

Fig. 3 (*a*) Schematic depiction of the physical force balance used to determine the intrasheet force at the colony midline. (*b*) Variation of the intrasheet force at the colony midline as a function of the orientation of the midline for the colony shown in Figs. 1(*b*) and 1(*c*). (*c*) The maximum and minimum sheet force in a colony normalized by its average sheet force across all orientations ($n = 6$ colonies).

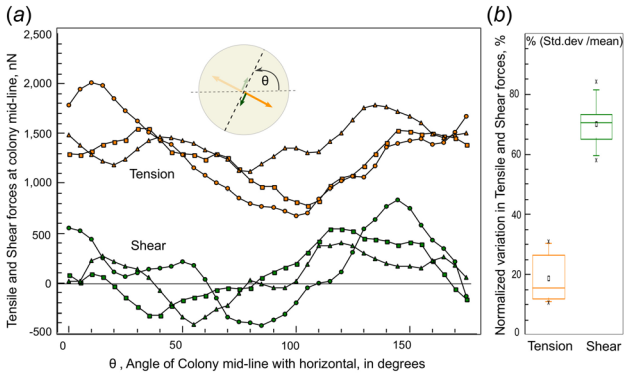

Fig. 4 (*a*) Variation of the tensile and shear components of the endogenous sheet force at the colony midline with the orientation of the midline, shown for three representative colonies with similar average sheet force. (*b*) Normalized variation in the sheet tension and shear within each colony in % ($n = 6$ colonies).

regions across the colony (pooled from $n = 6$ epithelial colonies). Next, in order to be able to apply TFIM, the vector sum of traction forces exerted by the cell colony should vanish (or be close to zero, subject to experimental error). We thus determined the vector sum of traction forces as well as the scalar sum (sum of the magnitudes) of traction forces exerted by the cell colonies (Fig. 2(*b*)). The magnitude of the ratio of the vector sum to the scalar sum of traction forces under the colony was $5 \pm 2\%$, comparable to that for the case of single cells or cell pairs [9].

Traction force imbalance method is premised on the balance between (the reaction to) traction forces exerted by the substrate on the part of the cell island under consideration and the endogenous forces exerted on this part of the cell island by the rest of the cell island [9]. Using TFIM, we sought to determine the endogenous sheet force exerted at the colony midline by one half of the colony on the other. Figure 3(*a*) illustrates the external forces acting on one half of the cell colony and the force-balancing principle underlying TFIM as applied to the colony. However, as evident in Fig. 3(*a*), the orientation of the midline can vary over 180 deg (i.e., the angle of the midline with the horizontal can be anywhere between 0 deg and 180 deg). Thus, we calculated the endogenous sheet force within the colony as a function of the orientation of the midline. For the colony shown in Fig. 1(*b*), we found that, remarkably, the endogenous sheet force (which was largely perpendicular to the midline, as mentioned further below) varied between a minimum of 700 ± 310 nN to a maximum of 2060 ± 310 nN as a function of the midline orientation (Fig. 3(*b*)) (see Sec. 2 for method of error estimation). Thus, the range of variation of the endogenous sheet force was comparable to the average sheet force of the colony (1330 nN, averaged over all midline orientations). For $n = 6$ colonies, the average endogenous sheet force at the colony midline, averaged over all orientations for each colony, was found to be 1310 ± 400 nN (see Sec. 2 for method of error estimation) and the maximum and minimum endogenous sheet force differed, on average, by 63% of the average sheet force of each colony (Fig. 3(*c*)).

In order to further explore the nature of the endogenous sheet force, we resolved it into tensile and shear components (as schematically depicted in Fig. 4(*a*) inset). Figure 4(*a*) shows the variation of the tensile and shear components with the midline orientation in three separate colonies with similar endogenous sheet forces. We found that, first, the endogenous sheet force is largely tensile in nature (i.e., the sheet force is largely perpendicular to the corresponding colony midline). Second, although smaller, whole colony-level shear forces persist at the midline. As evident in Fig. 4(*a*), the absolute variation in the tensile and shear forces was comparable. But since the shear forces are smaller in magnitude, the normalized variation (standard deviation/mean) in shear forces far exceeded that in the sheet tension at the midline (Fig. 4(*b*), $n = 6$ colonies). Thus, even though the net shear force vanished for specific orientations of the midline, they persist at the colony level in general, with an average magnitude of about one-fifth that of the sheet tension.

To demonstrate that the traction forces as well as the intrasheet tension that we determined here are ultimately due to cell-generated contractility and are not simply an experimental artifact, we determined their dependence on Rho-kinase activity. Rho-kinase is a Rho-GTPase effector that indirectly promotes myosin activity and hence contractility [23]. We used Y27632, a pharmacological inhibitor of Rho-kinase to reduce cell contractility and tested the effect of this on the measured traction and endogenous sheet forces. As shown in Fig. 5(*a*), treatment with 50 μM Y27632 for 1 h reduced the traction forces to near-background levels. The anisotropic endogenous sheet forces also concomitantly reduced drastically (Fig. 5(*b*)). For $n = 4$ colonies, 1 h of treatment with Y27632 reduced the endogenous sheet forces by $79 \pm 5\%$.

Since we used the Boussinesq solution in traction force calculations, we finally wanted to assess whether the finite thickness of the substrate (that varied between 150 and 200 μm) influenced the central result of this paper. To do this, we performed finite element method (FEM) computations taking into account finite substrate thickness (see Sec. 2) and compared this with the Boussinesq solution. As shown in Fig. 6(*a*), the traction heat map of the same colony as in Fig. 1(*b*) was largely similar. More importantly, the FEM results (that took finite substrate thickness into account) also yielded similar anisotropy in the endogenous sheet tension (Fig. 6(*b*)). Comparison of the sheet tension calculated using traction values obtained from the Boussinesq solution and the traction values obtained using the FEM with finite substrate thickness showed that they differed by ~15%, comparable to the error in the computation of the sheet tension itself. Thus, the key finding of this work (i.e., anisotropy of the sheet force, which is predominantly tensile) was also exhibited by the sheet force calculated using the traction forces from the FEM computation which took finite substrate thickness into account.

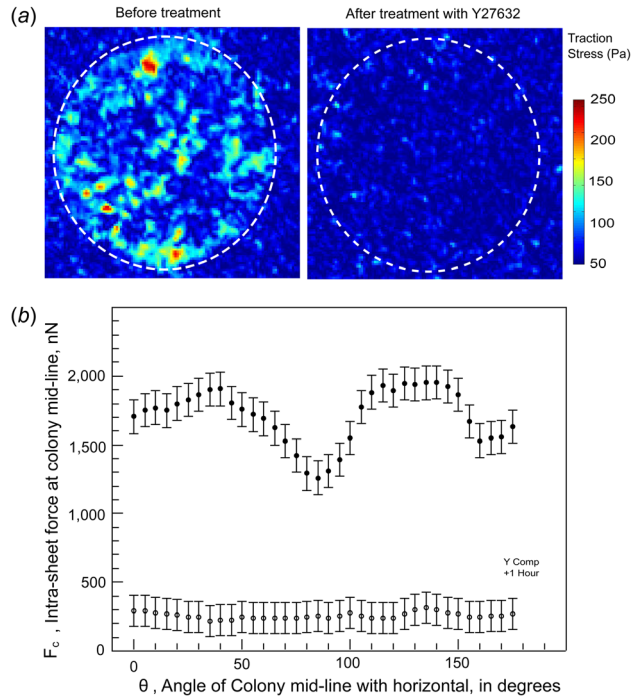

Fig. 5 Traction and sheet forces are Rho-kinase sensitive. (*a*) Heat map representation of the traction stress under the MDCK cell colony before and after 1 h of treatment with 50 μM of the Rho-kinase inhibitor Y27632. (*b*) Variation of the intrasheet force at the colony midline as a function of the orientation of the midline before and after 1 h treatment with Y27632.

4 Discussion

We found that the endogenous sheet forces within large epithelial colonies display high tension and anisotropy. The average magnitude of the endogenous sheet tension normalized by the sheet diameter, i.e., the average sheet tension per unit length that we find for the colony, is 2.5 ± 0.8 nN/μm. This is comparable to a similar measure recently reported for a unidirectionally expanding MDCK sheet along the direction of expansion [24] and to the local cell–cell tension calculated in much smaller islands with the assumption of uniform cell island mechanical properties [25]. This suggests that even quiescent epithelial cell colonies (not engaged in directed migration) are in a highly tense state and this tensional state may be expected to regulate multiple biochemical processes that maintain homeostasis of the cell colony.

It is worth noting that, unlike for cell pairs [8,9,14], the endogenous sheet tension within the colony determined here using TFIM involves contributions from tension both perpendicular and parallel to individual cell–cell contacts, as the cell–cell contacts themselves are multiply oriented in an unrestrained manner near the colony midline. Thus, the endogenous sheet tension reported here is a useful metric to characterize the tensional state of an epithelial colony and it reflects tension transmitted through cell–cell contacts and the cells themselves with a colony.

The large circular epithelial cell colony and its sheet forces determined here using TFIM can help bridge the gap between studies involving cell pairs/small islands [8,9,15] where the extent of free boundary is comparable to the extent of cell–cell contacts and studies of colonies and expanding monolayers [25,26] where uniform cell mechanical properties have been assumed. While seminal studies of expanding monolayers [12,26] have the advantage of obtaining local forces, it involves approximations at the frame boundaries and the assumption of uniform cell mechanical properties [26]. While our current approach has the disadvantage that it does not obtain local forces, but only average sheet forces (which implies that variations along the midline cannot be captured), it has the advantage of obtaining data from a single frame without similar assumptions at the frame boundaries or assumption of uniform cell mechanical properties. Thus, our approach here provides an alternative means to obtain useful mechanical readouts from cell collectives, but has the disadvantage that local forces are not obtained. Our experimental model also has a free boundary, but the effect of the boundary is less significant than that for small cell islands in that large traction stresses are no longer limited to the cell island periphery here (as depicted in Fig. 2(*a*)). Comparison of the average sheet tension obtained here ($\sim$2.5 nN/μm) with a corresponding average measure reported [24] in a unidirectionally expanding monolayer of the same cell type (average of $\sim$2.7 nN/μm) leads us to estimate that the effect due to the free boundary may be causing a difference in the vicinity of 10%. However, sheet tension during individual time points of monolayer expansion [24] varied by as much as -12% to $+28\%$, relative to the average value reported here. Further studies with even larger colonies and monolayers should enable greater comparison between, and integration of, conclusions from the earlier studies and the extent to which anisotropies in sheet tension diminish or persist.

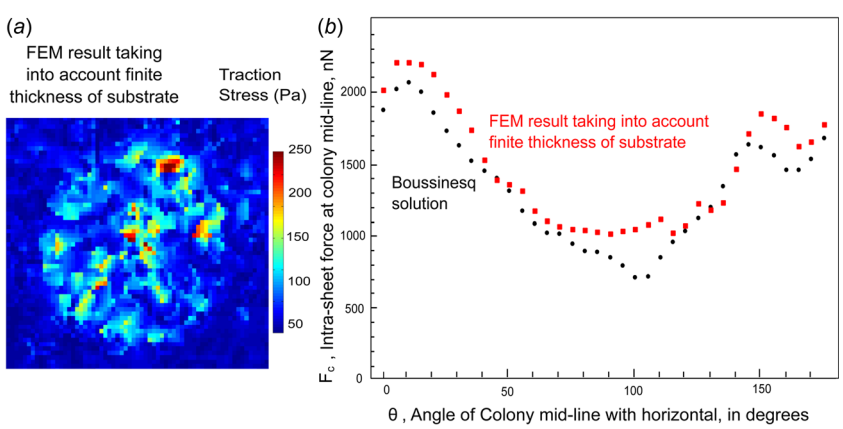

Fig. 6 (*a*) Heat map representation of the traction stresses under the colony computed using a finite element model of the substrate as a linear, isotropic elastic medium of finite thickness (of 150 μm). Compare with the Boussinesq solution in Fig. 1(*c*). (*b*) Comparison of the intrasheet force at the midline obtained using the Boussinesq solution and the FEM result considering the finite thickness of the substrate. Estimated errors (not shown in the figure) in the Boussinesq solution sheet force are 310 nN and in the FEM results sheet force are 670 nN.

What might cause the directional variation in the endogenous sheet forces observed here? When we quantified the variation in the number of cells in each octant of each colony, we found that the standard deviation in cell number per octant for each colony was in the range of 10–20%. We could also detect no significant spatial changes in cell extracellular matrix deposition when we assayed for collagen or fibronectin using immunofluorescence (the immunofluorescence was dominated by the cytoplasmic pool, data not shown). While we cannot conclusively rule out spatial variation in cell density or extracellular matrix as contributing factors to the orientation dependence of the sheet tension, we propose that cell-to-cell heterogeneities in force generation and transmission brought about by variations in the architecture and composition of the cytoskeletal, adhesive, and contractile apparatus may well play a major role. Just as determination of the endogenous force at a single cell–cell contact offers insight into the dynamic organization of a cell pair [14], knowledge of colony-level forces and specific biochemical factors inside the cells that lead to their directional variation can be expected to yield insights into larger scale multicellular rearrangements.

Acknowledgment

We thank Benedikt Sabass and Ulrich Schwarz for the script to reconstruct traction stresses.

Funding Data

- National Institute of General Medical Sciences (Grant No. 1R15GM116082).
- Thomas F. and Kate Miller Jeffress Memorial Trust (Grant No. 15-339).

References

[1] Heisenberg, C. P., and Bellaïche, Y., 2013, "Forces in Tissue Morphogenesis and Patterning," Cell, **153**(5), pp. 948–962.

[2] Lecuit, T., Lenne, P.-F., and Munro, E., 2011, "Force Generation, Transmission, and Integration During Cell and Tissue Morphogenesis," Annu. Rev. Cell Dev. Biol., **27**(1), pp. 157–184.

[3] Martin, A. C., Gelbart, M., Fernandez-Gonzalez, R., Kaschube, M., and Wieschaus, E. F., 2010, "Integration of Contractile Forces During Tissue Invagination," J. Cell Biol., **188**(5), pp. 735–749.

[4] Meng, W., and Takeichi, M., 2009, "Adherens Junction: Molecular Architecture and Regulation," Cold Spring Harbor Perspect. Biol., **1**(6), p. a002899.

[5] Bambardekar, K., Clement, R., Blanc, O., Chardes, C., and Lenne, P. F., 2015, "Direct Laser Manipulation Reveals the Mechanics of Cell Contacts In Vivo," Proc. Natl. Acad. Sci. U.S.A., **112**(5), pp. 1416–1421.

[6] Campas, O., Mammoto, T., Hasso, S., Sperling, R. A., O'Connell, D., Bischof, A. G., Maas, R., Weitz, D. A., Mahadevan, L., and Ingber, D. E., 2014, "Quantifying Cell-Generated Mechanical Forces Within Living Embryonic Tissues," Nat. Methods, **11**, pp. 183–189.

[7] Borghi, N., Sorokina, M., Shcherbakova, O. G., Weis, W. I., Pruitt, B. L., Nelson, W. J., and Dunn, A. R., 2012, "E-cadherin Is Under Constitutive Actomyosin-Generated Tension That Is Increased at Cell-Cell Contacts Upon Externally Applied Stretch," Proc. Natl. Acad. Sci., **109**(31), pp. 12568–12573.

[8] Liu, Z., Tan, J. L., Cohen, D. M., Yang, M. T., Sniadecki, N. J., Ruiz, S. A., Nelson, C. M., and Chen, C. S., 2010, "Mechanical Tugging Force Regulates the Size of Cell-Cell Junctions," Proc. Natl. Acad. Sci. U.S.A., **107**(22), pp. 9944–9949.

[9] Maruthamuthu, V., Sabass, B., Schwarz, U. S., and Gardel, M. L., 2011, "Cell-ECM Traction Force Modulates Endogenous Tension at Cell-Cell Contacts," Proc. Natl. Acad. Sci. U.S.A., **108**(12), pp. 4708–4713.

[10] Muhamed, I., Chowdhury, F., and Maruthamuthu, V., 2017, "Biophysical Tools to Study Cellular Mechanotransduction," Bioengineering, **4**(1), p. 12.

[11] Ng, M. R., Besser, A., Brugge, J. S., and Danuser, G., 2014, "Mapping the Dynamics of Force Transduction at Cell-Cell Junctions of Epithelial Clusters," eLife, **3**, p. e03282.

[12] Tambe, D. T., Hardin, C. C., Angelini, T. E., Rajendran, K., Park, C. Y., Serra-Picamal, X., Zhou, E. H., Zaman, M. H., Butler, J. P., Weitz, D. A., Fredberg, J. J., and Trepat, X., 2011, "Collective Cell Guidance by Cooperative Intercellular Forces," Nat. Mater., **10**(6), pp. 469–475.

[13] Tang, X., Tofangchi, A., Anand, S. V., and Saif, T. A., 2014, "A Novel Cell Traction Force Microscopy to Study Multi-Cellular System," PLoS Comput. Biol., **10**(6), p. e1003631.

[14] Maruthamuthu, V., and Gardel, M. L., 2014, "Protrusive Activity Guides Changes in Cell-Cell Tension During Epithelial Cell Scattering," Biophys. J., **107**(3), pp. 555–563.

[15] Mertz, A. F., Banerjee, S., Che, Y., German, G. K., Xu, Y., Hyland, C., Marchetti, M. C., Horsley, V., and Dufresne, E. R., 2012, "Scaling of Traction Forces With the Size of Cohesive Cell Colonies," Phys. Rev. Lett., **108**(19), p. 198101.

[16] Wang, N., Tolic-Norrelykke, I. M., Chen, J., Mijailovich, S. M., Butler, J. P., Fredberg, J. J., and Stamenovic, D., 2002, "Cell Prestress. I. Stiffness and Prestress Are Closely Associated in Adherent Contractile Cells," Am. J. Physiol. Cell Physiol., **282**(3), pp. C606–C616.

[17] Vignaud, T., Ennomani, H., and Thery, M., 2014, "Polyacrylamide Hydrogel Micropatterning," Methods Cell Biol., **120**, pp. 93–116.

[18] Martiel, J. L., Leal, A., Kurzawa, L., Balland, M., Wang, I., Vignaud, T., Tseng, Q., and Théry, M., 2015, "Measurement of Cell Traction Forces With ImageJ," Methods Cell Biol., **125**, pp. 269–287.

[19] Butler, J. P., Tolic-Norrelykke, I. M., Fabry, B., and Fredberg, J., 2002, "Traction Fields, Moments, and Strain Energy That Cells Exert on Their Surroundings," Am. J. Physiol. Cell Physiol., **282**(3), pp. C595–C605.

[20] Plotnikov, S. V., Sabass, B., Schwarz, U. S., and Waterman, C. M., 2014, "High-Resolution Traction Force Microscopy," Methods Cell Biol., **123**, pp. 367–394.

[21] Sabass, B., Gardel, M. L., Waterman, C. M., and Schwarz, U. S., 2008, "High Resolution Traction Force Microscopy Based on Experimental and Computational Advances," Biophys. J., **94**(1), pp. 207–220.

[22] Schwarz, U. S., Balaban, N. Q., Riveline, D., Bershadsky, A., Geiger, B., and Safran, S. A., 2002, "Calculation of Forces at Focal Adhesions From Elastic Substrate Data: The Effect of Localized Force and the Need for Regularization," Biophys. J., **83**(3), pp. 1380–1394.

[23] Kimura, K., Ito, M., Amano, M., Chihara, K., Fukata, Y., Nakafuku, M., Yamamori, B., Feng, J., Nakano, T., Okawa, K., Iwamatsu, A., and Kaibuchi, K., 1996, "Regulation of Myosin Phosphatase by Rho and Rho-Associated Kinase (Rho-Kinase)," Science, **273**(5272), pp. 245–248.

[24] Vincent, R., Bazellieres, E., Perez-Gonzalez, C., Uroz, M., Serra-Picamal, X., and Trepat, X., 2015, "Active Tensile Modulus of an Epithelial Monolayer," Phys. Rev. Lett., **115**(24), p. 248103.

[25] Casares, L., Vincent, R., Zalvidea, D., Campillo, N., Navajas, D., Arroyo, M., and Trepat, X., 2015, "Hydraulic Fracture During Epithelial Stretching," Nat. Mater., **14**(3), pp. 343–351.

[26] Tambe, D. T., Croutelle, U., Trepat, X., Park, C. Y., Kim, J. H., Millet, E., Butler, J. P., and Fredberg, J. J., 2013, "Monolayer Stress Microscopy: Limitations, Artifacts, and Accuracy of Recovered Intercellular Stresses," PLoS One, **8**(2), p. e55172.